Impedance-Based Stability Evaluation for Multibus DC Microgrid Without Constraints on Subsystems

Leng, Minrui; Zhou, Guohua; Li, Haoze; Xu, Guodong; Blaabjerg, Frede; Dragičević, Tomislav

Published in:
I E E E Transactions on Power Electronics

DOI (link to publication from Publisher):
10.1109/TPEL.2021.3093372

Publication date:
2022

Document Version
Accepted author manuscript, peer reviewed version

Impedance-Based Stability Evaluation for Multibus DC Microgrid Without Constraints on Subsystems

Minrui Leng, *Student Member*, *IEEE*, Guohua Zhou, *Senior Member*, *IEEE*, Haoze Li, Guodong Xu, Frede Blaabjerg, *Fellow*, *IEEE*, Tomislav Dragičević, *Senior Member*, *IEEE*

***Abstract* – Multibus dc microgrids, which combine renewable energy sources, energy storage systems and loads, have voltage stability requirement, which solicits increasing research attention in practice. Potentially complex architectures of the multibus dc microgrids make it difficult to evaluate the stability using the conventional stability criteria. In this paper, some constraints related to the conventional stability criteria, such as right-half-plane (RHP) poles or zeros in the subsystems are discussed. Further, an impedance-based stability criterion is proposed in the light of generalized bode plots for multibus dc microgrids. The configuration of the multibus dc microgrid is simplified by adopting generalized voltage source, generalized current source and two-port model. Then, impedances or admittances for each bus port can be derived, which are helpful for assessing the stability of the system. Using the proposed stability criterion, the stability of each bus port in the multibus dc microgrid can be evaluated separately. The proposed stability method considers the number of RHP pole of the open-loop transfer function for the system so the stability of the system consists of subsystems with RHP pole and zero can be analyzed correctly. Moreover, the intermittent bus converter connected with neighboring dc microgrid can be regarded as an extension unit. Then the proposed method can be easily extended and is acting as a generalized approach for different configurations, i. e. single-bus dc mirogrid, or a cluster of dc microgrids. Experiments are done to validate the effectiveness of the proposed criterion.**

***Index Terms*—Multibus dc microgrid, RHP poles and zeros, impedance-based stability criterion, generalized bode plots, extension unit.**

I. INTRODUCTION

NOWADAYS, the revolutionary changes in the electric power system, including the penetration of renewable energy sources, the distributed allocation of generation and the increasing participation of consumers, make an increasing popularity of microgrid [1-4]. Owing to higher efficiency, a more natural interface to many types of renewable energy sources and hybrid energy storage as well as better compliance with consumer electronics, dc microgrid is regarded more attractive for plenty of users [2], such as electric ships [5], vehicular electric power systems [6], dc-powered homes [7], etc.

Different configurations of the dc microgrid should be considered according to practical requirements. Since it is common that different types of modern consumer electronic appliances are operated on distinctive voltage levels, multibus microgrid including multiple buses with different voltages has potential in industry [8]. The multibus microgrid is extended from a single-bus topology, providing increased energy efficiency, power density, and reliability, at possibly lower installation and operation costs [9-11]. However, with integration of numerus power converters and many dc buses, stability assessment of the system is an urgent and worthwhile challenge because interactions among different power converters may cause instability, which threatens the operation of the whole system.

Most recent works related to stability analysis are based on small signal models. For cascaded systems, the impedance-based method is regarded as an effective way to analyze the stability, which can be dated back to design the input-filter for regulated converters proposed by Middlebrook in 1976 [12]. The Middlebrook criterion claims that the stability of cascaded system will be guaranteed if both subsystems are stable, and the minor loop gain, defined as the ratio of the source converter's output impedance and load converter's input impedance, does not exit the unity circle on the complex plane. However, only the magnitudes of the subsystem input and output impedances are considered, resulting in a conservative design owing to the demand of infinite phase margin. Later on, the gain and phase margin criterion [13] is proposed, which specifies a forbidden region in the s-plane for the minor loop gain, providing sufficient gain and phase margins and loosening the conservativeness of the Middlebrook criterion [14]. After that, the opposing argument criterion [15-16], the energy source analysis consortium criterion [17] and the root exponential stability criterion [18] are proposed, defining various forbidden regions for polar plot of the minor loop gain, further reducing the conservativeness [19]. These criteria are assuming a given power flow direction by defining a source subsystem and a load subsystem, suffering inapplicability if

Manuscript received January 27, 2021; revised May 6, 2021; accepted June 14, 2021. This work was supported in part by the National Natural Science Foundation of China under Grant 61771405, the Sichuan Science and Technology Program under Grant 2019JDTD0003, and the State Scholarship Fund of China Scholarship Council (CSC). (*Corresponding author: Guohua Zhou*)

M. Leng is with the College of Electrical Engineering, Sichuan University, Chengdu, 610065, China, and also with School of Electrical Engineering, Southwest Jiaotong University, Chengdu 611756, China. (e-mail: mrleng_pece@163.com)

G. Zhou, H. Li, and G. Xu are with School of Electrical Engineering, Southwest Jiaotong University, Chengdu 611756, China (e-mail: ghzhou-swjtu@163.com; lihao0ze@163.com; xgd_pece@163.com.

F. Blaabjerg is with the Department of Energy Technology, Aalborg University, Aalborg 9220, Denmark (e-mail: fbl@et.aau.dk).

T. Dragičević are with the Department of Electrical Engineering, Technical University of Denmark (DTU), Denmark, (email: tomdr@elektro.dtu.dk).

the power flow is reversed, i.e. if the operation of source subsystem and load subsystem are changed.

However, in a complex system like dc microgrid, photovoltaics and energy storage are widely included [20-21], which introduces different operation modes and power flow directions, making it difficult to evaluate the stability. Aiming at this problem, subsystems in the system are classified into a bus voltage-controlled converter (BVCC) or a bus current-controlled converter (BCCC) [22]. Then, a unified form regardless of structures and operating modes of the system can be redefined, where stability can be analyzed by testing the equivalent loop gain of the system based on the Nyquist criterion.

Except for the impedance-based criteria, the impedance-sum criteria [23-25] is also developed, which derives the closed-loop characteristic polynomial of the system, being analyzed by a Cauchy theorem or a Nyquist criterion.

The above stability methods are sharing the common precondition that subsystems should be stable, which means they should not have any right-half-plane (RHP) poles [26]. For system with multiple converters, the impedance ratio or the impedance sum is rearranged as a whole. As a result, the existing RHP zeros in subsystems may introduce RHP poles due to the inverse impedance. Therefore, these stability methods have constraints, which only apply to the systems without RHP poles or zeros in the subsystems.

Moreover, most of the aforementioned works are directing at systems with a single dc bus. For the stability analysis of multibus dc microgrid, it is more complex to account the intermediate bus converter (IBC), which acts as a voltage matching and power exchange unit [27-29], as shown in Fig.1. Evaluating the stability of multibus dc microgrid gains increasing concerns thanks to its popularity in recent years. By extending the passivity-based stability criterion and adopting the new concept of an allowable impedance region, stability for multibus distributed system is evaluated, from the perspective of system passivity [30]. The multibus distributed system is reduced to equivalent interacting source and load subsystem networks by looking into single 1-bus port, resulting in the equivalent 1-port network. Hence the impedances of subsystems cannot explicitly be specified and the stability margin cannot be designed intuitively. From the perspective of impedance ratio, [31] proposes an impedance-based criterion for distributed power system with multivoltage levels, which is extended from [22] and has constraints on the RHP poles or zeros in the subsystems. Moreover, it is centralized, and has two problems, one is high dimensionality and the other is that it is not suitable for plug-play applications.

This paper focuses on the stability assessment of multibus dc microgrids, and proposing an impedance-based stability method based on the generalized bode criterion even though there are RHP poles or zeros in the subsystems. Moreover, the stability of the multibus dc microgrid for each bus port can be analyzed separately, which can be extended to a single-bus dc microgrids and cluster of multiple dc microgrids. As a result, the proposed impedance-based stability method can solve the constraints of the existing impedance-based criterion and provides a generalized method for dc microgrids with different configurations.

This paper is organized as follows. Section II describes the equivalent form of the mutibus dc microgrid with two voltage levels. In Section III, simplification of the mutibus dc microgrid with two voltage levels is given. Section IV analyzes the stability of the mutibus dc microgrid with two voltage levels and extends it to other configurations. Section V gives a case study demonstrated at simulation and experimental results to verify the effectiveness of the proposed method. Finally, Section VI concludes the paper.

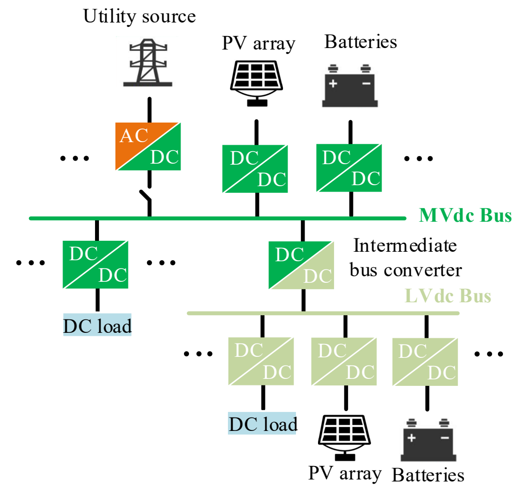

Fig. 1. Typical multibus dc microgrid with two voltage levels.

II. Equivalent Form of the Multibus DC Microgrid

A. Description of the Multibus DC Microgrid

The multibus dc microgrid typically comprises several different buses, providing power for commercial and residential applications, such as datacom centers, aircraft power systems, etc. The typical multibus dc microgrid is depicted in Fig. 1, where the dc microgrid with two voltage levels, a medium-voltage dc (MVdc) bus and a low-voltage dc (LVdc) bus, being used as an example. For each bus, there are PV arrays, batteries and loads connected. The different buses are further linked by the IBC.

It should be noted that for the multibus dc microgrid, there are different operation modes due to the different energy flow. Moreover, the actual modes of the IBC are depended on various dc bus operating modes [32]. Therefore, operating modes of each bus should be investigated firstly.

Denoting P_{pv} and P_o are the output power of the PV array and load converter respectively.

Mode I: If $P_{pv} < P_o$, it means that the PV array provides as much as possible energy to the load by a maximum power point tracking (MPPT) algorithm, which acts as a power source. The batteries and a bidirectional dc-dc converter are used to make up the energy by regulating bus voltage, which can be regarded as a voltage source.

Mode II: If $P_{pv} > P_o$ by a small margin, the loads can be fully fed by the PV array. The small extra energy is adopted to charge the battery which still regulates the bus voltage.

Therefore, the PV array and corresponding converter are denoted as a power source while the battery and a bidirectional dc-dc converter are viewed as a voltage source.

Mode III: If $P_{\mathrm{pv}} > P_{\mathrm{o}}$, in case of continuously good sunshine, the output voltage of PV array is up to the bus voltage. The PV array can provide sufficient energy to the loads and charge batteries with a constant current, which then regulates the bus voltage instead of adopting MPPT algorithm.

Mode IV: If $P_{\mathrm{pv}} > P_{\mathrm{o}}$ and the batteries are fully charged, the PV array still regulates the bus voltage, while the batteries are in floating charging to avoid self-discharge.

The operation mode of IBC is determined by each bus. For the MVdc bus port, the IBC can be regarded as a load because it generally absorbs power from the MVdc bus. From the perspective of LVdc bus port, the IBC can exchange power according to the specific modes of the bus.

As discussed above, there are different operating modes for each bus. Moreover, with the consideration of the IBC, as well as the connection of the two buses, the situations are pretty complicated.

B. Equivalent Form for the Multibus DC Microgrid

Considering some of the sources or loads may be connected to the bus directly instead of linking by converters in practical, definitions of BVCC and BCCC in [22] are extended to generalized voltage source (GVS) and generalized current source (GCS), respectively [33].

1) GVS refers to a subsystem which controls or affects its bus-side-port-voltage.
2) GCS refers to a subsystem which controls or affects its bus-side-port-current.

The Thevenin equivalent circuit and Norton equivalent circuit for GVS and GCS are shown in Fig. 2. In order to describe the system by a standard form regardless of its operation modes as well as simplify the analysis, equivalent form for each bus is arranged. Then, the multibus dc microgrid can be described as show Fig. 3.

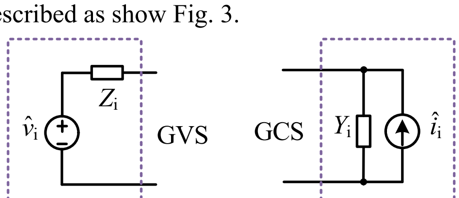

(a) (b)

Fig. 2. Thevenin equivalent circuit and Norton equivalent circuit for generalized voltage source (GVS)and generalized current source (GCS). (a) GVS. (b) GCS.

Considering the operating modes for the IBC, the complexity will be increased if it is classified as GVS or GCS. It is reasonable to use another model to represent the IBC because the IBC will not affect the operating modes for each bus ports. Therefore, a two-port model is adopted, providing some physical insight due to a Thevenin/Norton representation of the converter. Fig. 4 shows the equivalent form for the IBC by two-port model, where Y is the input admittance, H is the back current gain, Z is the output impedance, G is the audio-susceptibility.

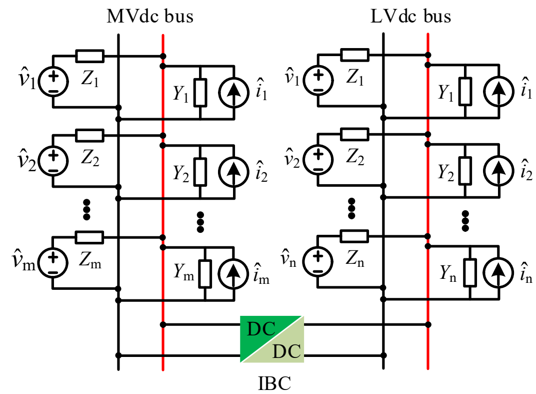

Fig. 3. Multibus dc microgrid described by GVS and GCS.

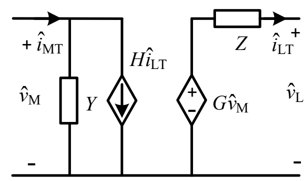

Fig. 4. Equivalent form of the IBC by two-port model.

III. Simplification of the Multibus DC Microgrid

As it can be seen from Fig. 3, there are two groups in each bus, consisting of the GVS group represented by the Thevenin equivalent circuits and the GCS group represented by the Norton equivalent circuits. To make it more concise, the two groups are combined respectively. As a result, on the basis of the equivalent forms for each bus as well as intermediate bus converter, the simplification of the multibus dc microgrid can be obtained. There are 4 possible simplified forms for the multibus dc microgrid, as shown in Fig. 5.

Fig. 5 is obtained by further simplifying the equivalent circuits of the two buses based on Thevenin or Norton theory. As a result, there are 4 possible forms: 1) N-N system, the MVdc bus and the LVdc bus are simplified by the Norton equivalent circuits, as shown in Fig. 5(a); 2) T-N system, the MVdc bus is simplified by the Thevenin equivalent circuits and the LVdc bus is simplified by the Norton equivalent circuits, as shown in Fig. 5(b); 3) T-T system, the MVdc bus and the LVdc bus are simplified by the Thevenin equivalent circuits, as shown in Fig. 5(c); 4) N-T system, the MVdc bus is simplified by the Norton equivalent circuits and the LVdc bus is simplified by the Thevenin equivalent circuits, as shown in Fig. 5(d). The impedances of GVS and admittances of GCS for MVdc bus (Z_{MGVS} and Y_{MGCS}) and LVdc bus (Z_{LGVS} and Y_{LGCS}) can be expressed as:

$$\begin{cases} Z_{\mathrm{MGVS}} = Z_1 \| Z_2 \| \cdots \| Z_{\mathrm{m}} \\ Y_{\mathrm{MGCS}} = \sum_{i=1}^{\mathrm{m}} Y_i \end{cases} \tag{1}$$

$$\begin{cases} Z_{\mathrm{LGVS}} = Z_1 \| Z_2 \| \cdots \| Z_{\mathrm{n}} \\ Y_{\mathrm{LGCS}} = \sum_{i=1}^{\mathrm{n}} Y_i \end{cases} \tag{2}$$

For N-N system, the admittance Y_{inM} from the MVdc bus port as well as the impedance Z_{oL} from the LVdc bus port can be derived as:

$$\begin{cases} Y_{\mathrm{inM}} = Y + \dfrac{GHY_{\mathrm{L}}}{1+ZY_{\mathrm{L}}} \\ Z_{\mathrm{oL}} = Z + \dfrac{GH\dfrac{1}{Y_{\mathrm{M}}}}{1+Y\dfrac{1}{Y_{\mathrm{M}}}} \end{cases} \tag{3}$$

where $Y_{\mathrm{L}} = Y_{\mathrm{inL}} = Y_{\mathrm{LGCS}} + \dfrac{1}{Z_{\mathrm{LGVS}}}$, $Y_{\mathrm{M}} = Y_{\mathrm{oM}} = Y_{\mathrm{MGCS}} + \dfrac{1}{Z_{\mathrm{MGVS}}}$.

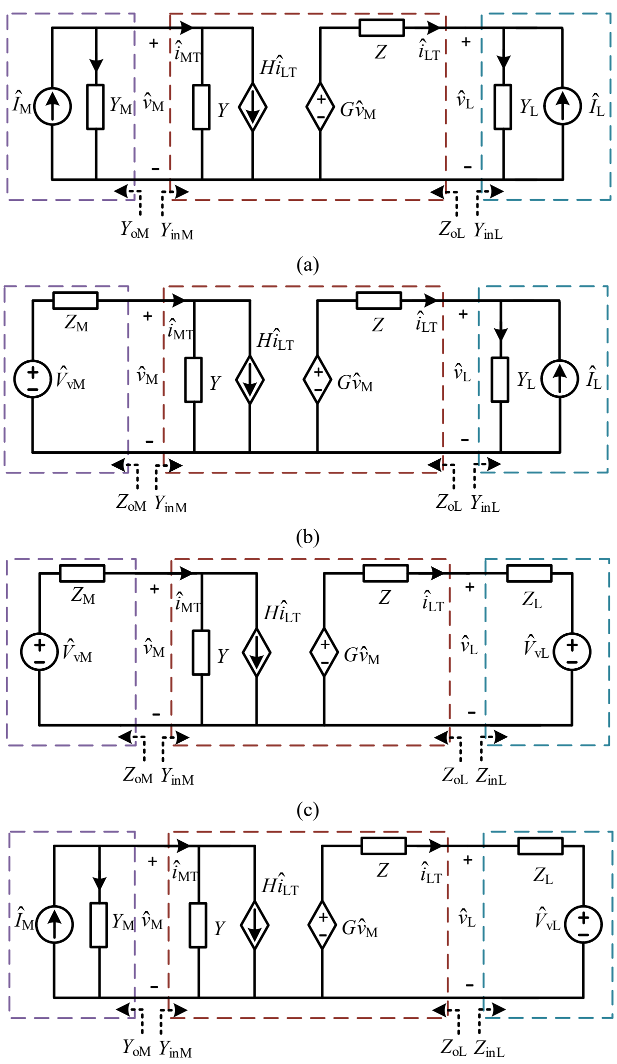

Fig. 5. Four possible simplified forms for the multibus dc microgrid. (a) N-N system. (b) T-N system. (c) T-T system. (d) N-N system.

For T-N system, the admittance Y_{inM} and the impedance Z_{oL} can be expressed as:

$$\begin{cases} Y_{\mathrm{inM}} = Y + \dfrac{GH}{\dfrac{1}{Y_{\mathrm{L}}}+Z} \\ Z_{\mathrm{oL}} = Z + \dfrac{GH}{\dfrac{1}{Z_{\mathrm{M}}}+Y} \end{cases} \tag{4}$$

where $Z_{\mathrm{M}} = Z_{\mathrm{oM}} = \dfrac{1}{\dfrac{1}{Z_{\mathrm{MGCS}}}+\dfrac{1}{Z_{\mathrm{MGVS}}}}$.

For T-T system, the admittance Y_{inM} and the impedance Z_{oL} can be expressed as:

$$\begin{cases} Y_{\mathrm{inM}} = Y + \dfrac{GH}{Z_{\mathrm{L}}+Z} \\ Z_{\mathrm{oL}} = Z + \dfrac{GH}{\dfrac{1}{Z_{\mathrm{M}}}+Y} \end{cases} \tag{5}$$

where $Z_{\mathrm{L}} = Z_{\mathrm{inL}} = \dfrac{1}{\dfrac{1}{Z_{\mathrm{LGVS}}}+\dfrac{1}{Z_{\mathrm{LGCS}}}}$.

For N-T system, the admittance Y_{inM} and the impedance Z_{oL} can be expressed as:

$$\begin{cases} Y_{\mathrm{inM}} = Y + \dfrac{GH}{Z_{\mathrm{L}}+Z} \\ Z_{\mathrm{oL}} = Z + \dfrac{GH}{Y_{\mathrm{M}}+Y} \end{cases} \tag{6}$$

Comparing (3) - (6), it can be seen that different forms of multibus dc microgrid can be equal to each other, and then the same expression for the admittance Y_{inM} from the MVdc bus port as well as the impedance Z_{oL} can be obtained.

Moreover, for each bus port, the minor loop gain can be obtained. Since the Y_{inM} and Z_{oL} are unchanged for different simplified forms, and the impedances and admittances for each bus, i. e. Z_{oM}, Z_{inL}, Y_{oM}, Z_{oL}, can be equivalent to each other, the four minor loop gains can also be equal mutually.

According to the simplified forms of the multibus dc microgrid, impedances or admittances for two buses can be obtained, offering information for stability assessment based on the minor loop gain. The stability of the two buses can be investigated separately, which can be analyzed from a point of decentralization.

IV. Stability Analysis

A. Reformulated Nyquist Criterion

The Nyquist criterion indicates that a system will be stable if the number Z of RHP pole of closed-loop transfer function equals to zero.

$$Z = P - N \tag{7}$$

where P is the number of RHP pole of the open-loop transfer function, and N is the number of times that the open-loop transfer function anti-clockwise encloses (-1, j0).

This criterion is useful in any system while it is complex to count the *N*, and it provides little physical insight into design. Existing stability criteria based on bode plot is widely used for stability assessment as well as stability improvement from the point of impedance specifications. However, it assumes that each subsystem is stable, and if there is any RHP zero in the subsystem, the RHP pole may be introduced to the open-loop transfer function due to the inverse. As a result, existing stability criteria come from a series specific cases of the Nyquist criterion, which can only be applied with restrictions on the systems. The main problems lie in that the *P* is overlooked. Moreover, the identification between the Nyquist diagram and bode plot should be considered in order to simplify the design.

Refs. [34-35] give a method to calculate *N* using bode plot instead of Nyquist diagram, like shown in Fig. 6, and making it possible to use bode criterion to accurately express the Nyquist criterion. Based on the concept, the Nyquist criterion can be reformulated as:

$$Z = P - 2\left(NC^{+} - NC^{-}\right) \tag{8}$$

where NC^+ is the number of crossing in the bode plot of the open-loop transfer function with phase $\pm n\cdot 180°$ (with *n* being an odd number) when the gain is greater than 0 dB and the phase increases; NC^- is the crossing number under the same conditions as NC^+ but with a decreasing phase.

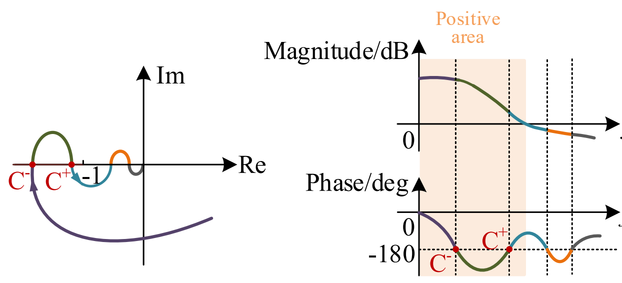

Fig. 6. Equivalent crossing in Nyquist diagram and bode plot. (a) Nyquist diagram. (b) Bode plot.

This concept in [35] is used to obtain the generalized bode criterion, which is also extended to multiple-input multiple-output systems [36] as well as analyzing the stability of interconnected converter systems [37].

B. Stability Prediction for a Multibus DC Microgrid

In order to evaluate the stability of multibus dc microgrid without constraints on the subsystems, i.e. subsystems with RHP zeros or RHP poles, the concept of crossing on Nyquist diagram using the expression of bode plot is adopted.

The process diagram to assess the stability of multibus dc microgrid is shown in Fig. 7. Steps A and B are described in Section II. Impedances or admittances from each bus port are obtained, which can be used for stability analysis according to the minor loop gain. Section II illustrates that the four minor loop gains for the four simplified forms of the multibus dc microgrid can also be mutually equal. Considering the clear physical meaning, the impedance-ratio for the MVdc bus port and admittance-ratio for the LVdc bus port are adopted as an example.

It should be noted that the Nyquist criterion supposes that the order of the numerator of the open-loop transfer function is lower than that of the denominator, or the frequency response of the transfer function reaches to zero (corresponding to the origin on the Nyquist diagram) at the infinite frequency [38]. Therefore, the frequency response of the minor loop gain for each bus port of the multibus dc microgrid should be defined as reaching to zero at the infinite frequency. The bode plots of the admittances Y_{oM} and Y_{inM}, impedances Z_{oL} and Z_{inL} should be depicted respectively to obtain the number of crossing point.

Step C gives identification of crossing from the point of the bode plot, avoiding counting them by the Nyquist diagram. As an example, Y_{small} and Y_{large} mean admittances that $|Y_{small}| < |Y_{large}|$ at the infinite frequency, the impedance-ratio can be defined as Y_{small} / Y_{large}, while $|Z_{small}| < |Z_{large}|$ at the infinite frequency, the impedance-ratio can be defined as Z_{small} / Z_{large}, which meets the assumption of the Nyquist criterion [37].

As it can be seen from Fig. 6, C^+ and C^- are denoted as the crossing points with the phase $\pm n\cdot 180°$counted on the bode plot when the phase increasing and decreasing and they are valid if the gain is greater than 0 dB. When it comes to the impedance-ratios Y_{small} / Y_{large} and Z_{small} / Z_{large}, as shown in Fig. 8, C^+ means the crossing point in the bode plot of the Y_{small} or Z_{small} with phase $\angle Y_{large} \pm n\cdot 180°$ or $\angle Z_{large} \pm n\cdot 180°$ if the phase increases when the gain of Y_{small} or Z_{small} is greater than Y_{large} or Z_{large}, denoted as positive area. C^- means the crossing point counted under the same conditions as C^+ but with a decreasing phase.

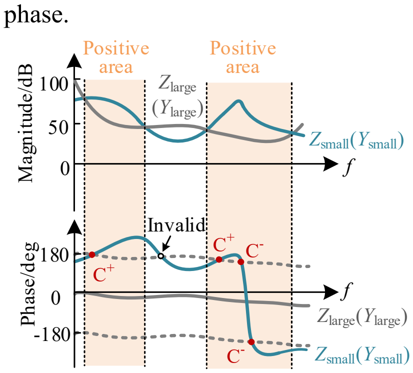

Fig. 8. Crossing of the Y_{small} / Y_{large} and Z_{small} / Z_{large} in bode plot.

After investigating the crossing numbers of the impedance-ratios, the stability can be predicted in step D, where the numbers of RHP poles in the impedance-ratios should also be acquired. The RHP poles in the impedance-ratios can be calculated as $P(Y_{small} / Y_{large}) = P_o(Y_{small}) + Z_e(Y_{large})$ or $P(Z_{small} / Z_{large}) = P_o(Z_{small}) + Z_e(Z_{large})$, where Z_e denotes the RHP zeros. The numbers of RHP poles or RHP zeros can be identified by the pole-zero maps or observing the slope of gains and phase change from the bode plot. According to (8), when $Z = 0$, the stability of multibus dc microgrid can be evaluated.

This article has been accepted for publication in a future issue of this journal, but has not been fully edited. Content may change prior to final publication. Citation information: DOI 10.1109/TPEL.2021.3093372, IEEE Transactions on Power Electronics

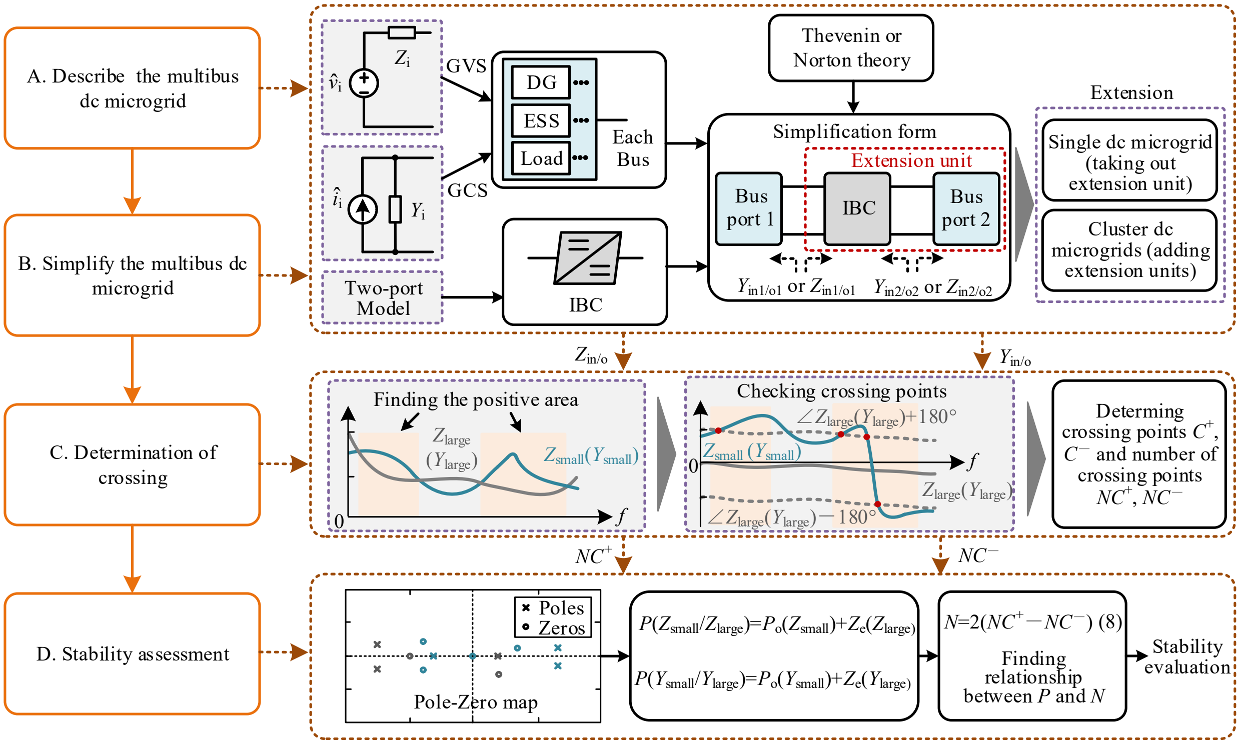

Fig. 7. Process diagram to assess the stability of multibus dc microgrid systematically.

C. Extension to Other Grid Configurations

For the multibus dc microgrid with two voltages like shown in Fig. 3, if there is no IBC connected, it can be regarded as two single-bus dc microgrids. Based on (1) and (2), the impedance-ratio or admittance-ratio of the single-bus dc microgrid can be further obtained, which are adopted to carry out the stability analysis, sharing the same stability prediction process with that of multibus dc microgrid as shown in Fig. 7.

Moreover, if there are other intermittent bus converters connected with neighboring dc microgrids, a dc microgrid cluster is constituted. The stability evaluation process of multibus dc microgrid can easily be extended. Fig. 9 shows a typical cluster of multiple dc microgrids. The configuration in Fig. 9 can also be developed to other application scenarios with more microgrids through intermittent bus converters or other active power electronic devices / converters.

According to step A in the process diagram in Fig. 7, the cluster of multiple dc microgrids can be described by GVS and GCS, as depicted in Fig. 10. Then intermittent bus converters are equivalented by two-port models like step B, and based on Thevenin or Norton theory where the simplified form for cluster of multiple dc microgrids can be expressed. As the same with that in multibus dc microgrid, the similar equivalence with Fig. 5(d) is adopted in Fig. 11. The admittances $Y_{\mathrm{in}jk}$, $Y_{\mathrm{in}kl}$ and the impedances $Z_{\mathrm{o}jk}$, $Z_{\mathrm{o}kl}$ can easily be obtained:

$$\begin{cases} Y_{\mathrm{in}jk} = Y_{jk} + \dfrac{G_{jk}H_{jk}}{\left(\dfrac{1}{Y_{\mathrm{in}kl}} + Z_k\right) + Z_{jk}} \\ Y_{\mathrm{in}kl} = Y_{kl} + \dfrac{G_{kl}H_{kl}}{Z_l + Z_{kl}} \end{cases} \tag{9}$$

$$\begin{cases} Z_{\mathrm{o}jk} = Z_{jk} + \dfrac{G_{jk}H_{jk}}{Y_j + Y_{jk}} \\ Z_{\mathrm{o}kl} = Z_{kl} + \dfrac{G_{kl}H_{kl}}{Y_{kl} + \left(\dfrac{1}{Z_k} + \dfrac{1}{Z_{\mathrm{o}jk}}\right)} \end{cases} \tag{10}$$

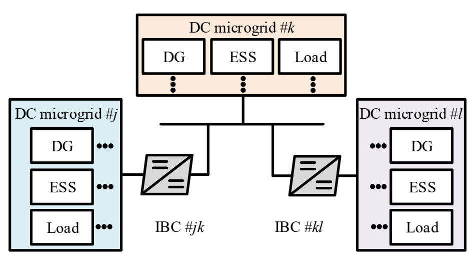

Fig. 9. A typical cluster dc microgrids with more than two systems.

Comparing Fig. 11 and Fig. 5(d), the difference is the adding of extension unit due to additional connection of an IBC and a neighbor dc microgrid. With the introduction of the extension unit, the admittance $Y_{\mathrm{in}kl}$ is brought in. By investigating the minor loop gains consisting of $Y_{\mathrm{in}kl}$, $Z_{\mathrm{o}jk}$, $Z_{\mathrm{in}k}$ from bus port #k, as well as impedance-ratio from bus port #j

and admittance-ratio from bus port #l, the stability for the cluster of multiple dc microgrids can be explored according to steps C and D in Fig. 7. If more microgrids through intermittent bus converters are connected, the method can be extended easily by paralleling the extension units to the corresponding bus port.

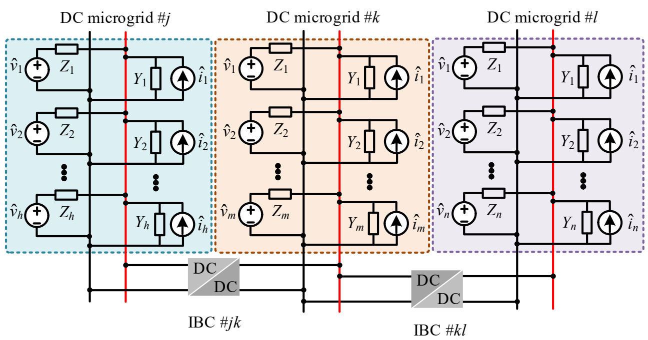

Fig. 10. Cluster of multiple dc microgrids described by GVS and GCS.

In conclusion, the proposed method can be extended to single-bus dc microgrid and cluster of multiple dc microgrids by taking out or adding the extension unit, acting as a generalized approach for different configurations without constraints on the subsystems. As a result, it is easy and simple for the system with penetration of a large amount of power converters and suitable for plug-play applications. According to the method, the stability of each bus port in the system can be evaluated separately.

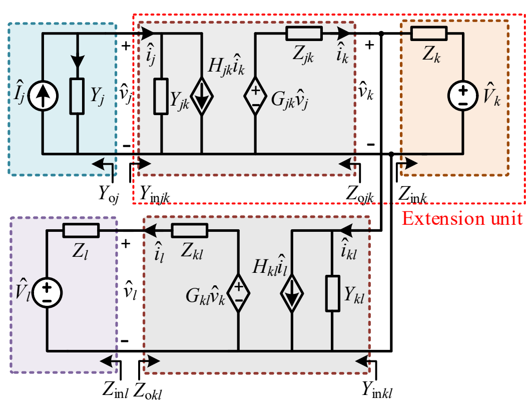

Fig. 11. Simplified form of the clustering multiple dc microgrids.

It should be noted that even though the method is simpler than many other conventional stability analysis methods, the impedances or admittances of the adding dc bus port should be calculated if other intermittent bus converters connected with neighboring dc microgrids are introduced. Therefore, the main disadvantage of the method is that with a very complex multibus dc microgrid, the calculation of the impedances or admittances of the adding bus ports are tedious. The bode plots and zero-pole maps of impedances or admittances for different bus ports should be provided which is a lengthy process.

V. CASE STUDY

Theoretical analysis and experiments are conducted to verify the validity of the proposed method. Fig. 12 depicts the topologies and controls of the analyzed system. The parameters are given in TABLE I. The unit 3 and unit 5 using the voltage control can be regarded as constant power loads (CPLs).

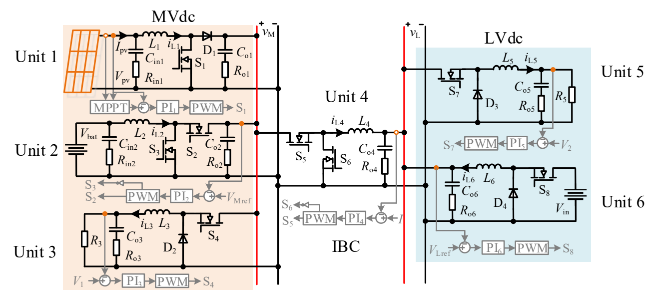

Fig. 12. Topologies and controls of the analyzed system.

According to the aforementioned analysis, the Y_{oM} and Y_{inM} for MVdc bus port, the Z_{oL} and Z_{inL} for LVdc bus port can be expressed as:

$$\begin{cases} Y_{\mathrm{oM}} = Y_{\mathrm{M}} = \dfrac{Z_{\mathrm{pv}} + Z_3}{Z_{\mathrm{pv}} Z_3} + \dfrac{1}{Z_2}, & Y_{\mathrm{inM}} = Y + \dfrac{GH}{Z_{\mathrm{L}} + Z} \\ Z_{\mathrm{inL}} = Z_{\mathrm{L}} = \dfrac{Z_6 Z_5}{Z_5 + Z_6}, & Z_{\mathrm{oL}} = Z + \dfrac{GH}{Y_{\mathrm{M}} + Y} \end{cases} \tag{11}$$

where Z_3, Z_{pv} and Z_5 are the input impedances of the Unit 1, Unit 3 and Unit 5 respectively; Z_2 and Z_6 are the output impedance of Unit 2 and Unit 6 respectively; Y, H, G, Z represent the two-port model of Unit 4, which can be obtained by using the small-signal circuit models of the source converter, the bidirectional converter and the load converter [22, 39-40].

TABLE I PARAMETERS OF THE SYSTEM

Parameters	L_1	C_{in1}	R_{in1}	C_{o1}	R_{o1}	V_{MPPT}
Values	100μH	100μF	0.1Ω	100μF	0.1Ω	15V
Parameters	L_2	C_{in2}	R_{in2}	C_{o2}	R_{o2}	V_{bat}
Values	100μH	100μF	0.1Ω	100μF	0.1Ω	24V
Parameters	V_{Mref}	L_3	C_{o3}	R_{o3}	V_1	L_4
Values	48V	200μH	100μF	0.1Ω	12V	200μH
Parameters	I	C_{o4}	R_{o4}	L_5	C_{o5}	R_{o5}
Values	1A	100μF	0.1Ω	200μH	100μF	0.1Ω
Parameters	V_2	L_6	C_{o6}	R_{o6}	V_{in}	V_{Lref}
Values	12V	200μH	100μF	0.1Ω	60V	24V

In order to verify the effectiveness of the stability evaluation method, different cases, including two stable buses, one stable bus and two unstable buses by changing the loads of MVdc bus and LVdc bus, are tested.

The bode plots and pole-zero maps for MVdc bus port and LVdc bus port when R_3 = 10 Ω, R_5 = 10 Ω; R_3 = 5 Ω, R_5 = 8 Ω; R_3 = 3 Ω, R_5 = 8 Ω; R_3 = 10 Ω, R_5 = 3 Ω, are depicted in Fig. 13 and Fig. 14. Based on the stability analysis shown in Fig. 7, the corresponding results are extracted in TABLE II.

As it can be seen in Fig. 13, the magnitude of Y_{oM} is larger than that of Y_{inM}, and the magnitude of Z_{oL} is larger than that of Z_{inL}. When R_3 = 10Ω and R_5 = 10Ω, there is a crossing point in the MVdc bus port and no crossing point in the LVdc bus port, which means that the $N = 2$ for the MVdc bus port and $N = 0$ for the LVdc bus port. In addition, the corresponding pole-zero maps shown in Fig. 14(a) indicate that the admittance Y_{oM} of the MVdc bus port has two RHP zeros and the admittance Y_{inM} of the MVdc bus port has no RHP pole, while the impedances Z_{oL} and Z_{inL} of the LVdc bus port have no RHP zero or pole. Therefore, both the MVdc bus port and the LVdc bus port satisfy equation (8), indicating that both the MVdc bus port and the LVdc bus port are stable.

When $R_3 = 5\Omega$, $R_5 = 8\Omega$; $R_3 = 3\Omega$, $R_5 = 5\Omega$; and $R_3 = 10\Omega$, $R_5 = 3\Omega$, there is a crossing point in the MVdc bus port, and a crossing point in the LVdc bus port. The differences of the above situations lie in the number of RHP poles and zeros. For $R_3 = 5\Omega$, $R_5 = 8\Omega$, the admittance Y_{oM} has two RHP zeros and the admittance Y_{inM} has one RHP pole while the impedances Z_{oL} has two RHP zeros, and Z_{inL} has no RHP pole, which indicates that the MVdc bus port is unstable and the LVdc bus port is stable. When $R_3 = 3\Omega$, $R_5 = 5\Omega$, both Y_{inM} and Z_{inL} have one RHP pole while both Y_{oM} and Z_{oL} have two RHP zeros, failing to satisfy (8). Therefore, both the MVdc bus port and the LVdc bus port are unstable. When $R_3 = 10\Omega$, $R_5 = 3\Omega$, there are oscillations in the MVdc bus voltage and the LVdc bus voltage because both Y_{inM} and Z_{inL} have one RHP pole while Y_{oM} has two RHP zeros and Z_{oL} has no RHP zero. As a result, with a relatively small load, the stability of the system will be degraded.

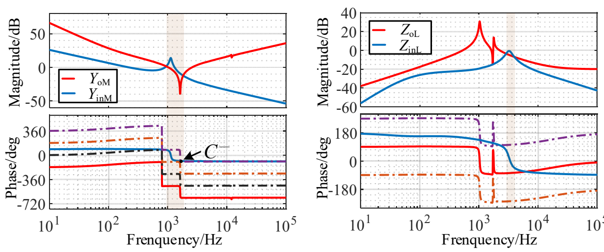

(a)

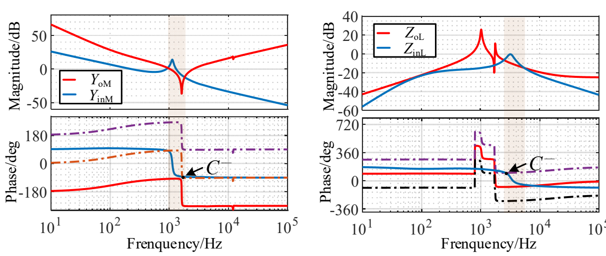

(b)

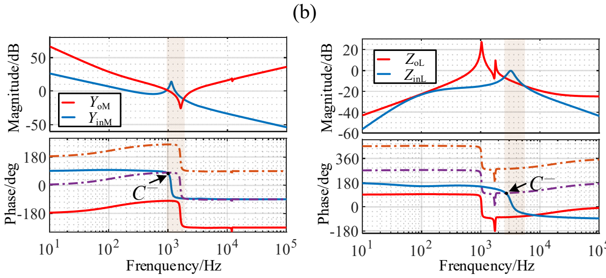

(c)

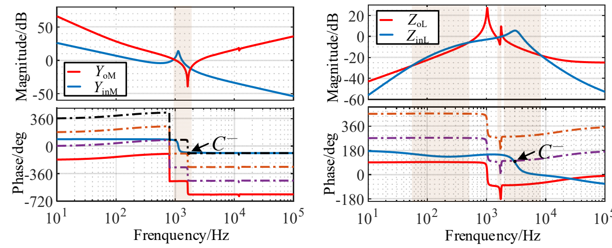

(d)

Fig. 13. Bode plots of Y_{inM}, Y_{oM}, Z_{inL}, Z_{oL} under different loads. (a) $R_3 = 10\ \Omega$, $R_5 = 10\ \Omega$. (b) $R_3 = 5\ \Omega$, $R_5 = 8\ \Omega$. (c) $R_3 = 3\ \Omega$, $R_5 = 5\ \Omega$. (d) $R_3 = 10\ \Omega$, $R_5 = 3\ \Omega$.

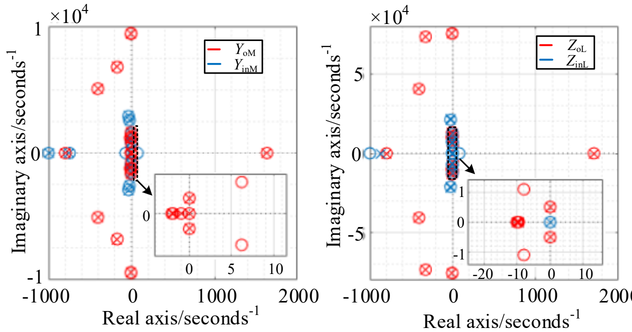

(a)

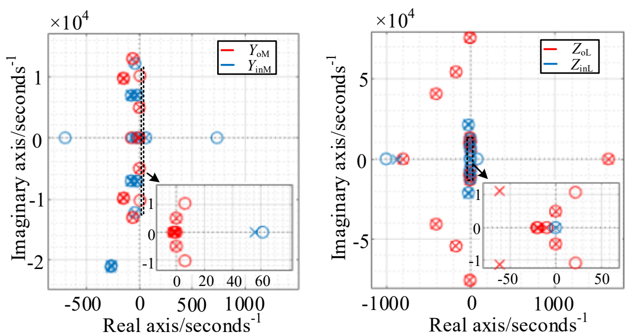

(b)

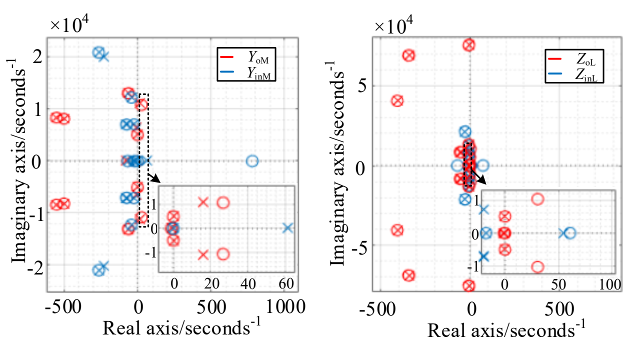

(c)

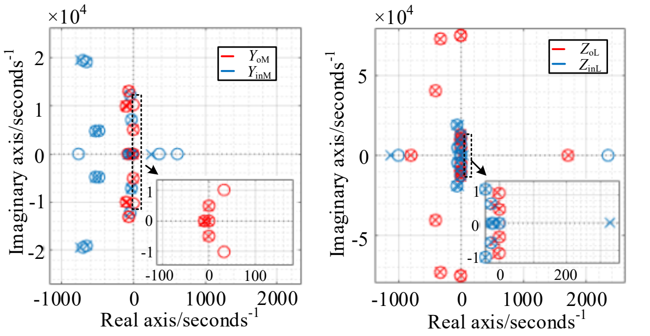

(d)

Fig. 14. Pole-zero maps of Y_{inM}, Y_{oM}, Z_{inL}, Z_{oL} under different loads. (a) R_3 = 10 Ω, R_5 = 10 Ω. (b) R_3 = 5 Ω, R_5 = 8 Ω. (c) R_3 = 3 Ω, R_5 = 5 Ω. (d) R_3 = 10 Ω, R_5 = 3 Ω.

TABLE II STABILITY BASED ON THE BODE PLOTS AND POLE-ZERO MAPS

Loads		R_3 = 10, R_5 = 10	R_3 = 5, R_5 = 8	R_3 = 3, R_5 = 5	R_3 = 10, R_5 = 3
MVdc	$P_o(Y_{small})$	$P_o(Y_{inM})$ = 0	$P_o(Y_{inM})$ = 1	$P_o(Y_{inM})$ = 1	$P_o(Y_{inM})$ = 1
	$Z_e(Y_{large})$	$Z_e(Y_{oM})$ = 2	$Z_e(Y_{oM})$ = 2	$Z_e(Y_{oM})$ = 2	$Z_e(Y_{oM})$ = 2
	N	2	2	2	2
	Stability	stable	unstable	unstable	unstable
LVdc	$P_o(Y_{small})$	$P_o(Z_{inL})$ = 0	$P_o(Z_{inL})$ = 0	$P_o(Z_{inL})$ = 1	$P_o(Z_{inL})$ = 1
	$Z_e(Y_{large})$	$Z_e(Z_{oL})$ = 0	$Z_e(Z_{oL})$ = 2	$Z_e(Z_{oL})$ = 2	$Z_e(Z_{oL})$ = 0
	N	0	2	2	2
	Stability	stable	stable	unstable	unstable

Steady state experimental waveforms for MVdc bus and LVdc bus under different R_5 and R_3 are presented in Fig. 15. It can be seen that with R_3 = 10 Ω, R_5 = 10 Ω, both the MVdc bus and LVdc bus are stable. It is observed from Fig. 15(b) that when R_3 = 5Ω, R_5 = 8Ω, there are very small oscillations existed in unit 2 and unit 3 at the MVdc bus port while there is barely no oscillation existed in unit 5 at the LVdc bus port. The MVdc bus voltage is unstable and LVdc bus voltage is stable. The oscillation in the MVdc bus port is very small and the unit 2 and unit 3 will absorb the oscillation. Even though there are interactions between the two bus ports, the very small oscillations in the MVdc bus port will have little effect on the LVdc bus port. Large oscillation occurs in MVdc bus and LVdc bus due to small R_5 or R_3, i.e. R_3 = 3 Ω or R_5 = 5 Ω. When R_5 is small, the oscillations occurring in the LVdc bus is more likely to be worse that in the MVdc bus.

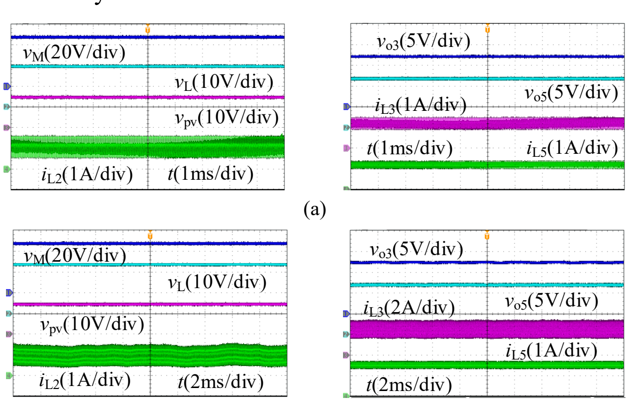

(b)

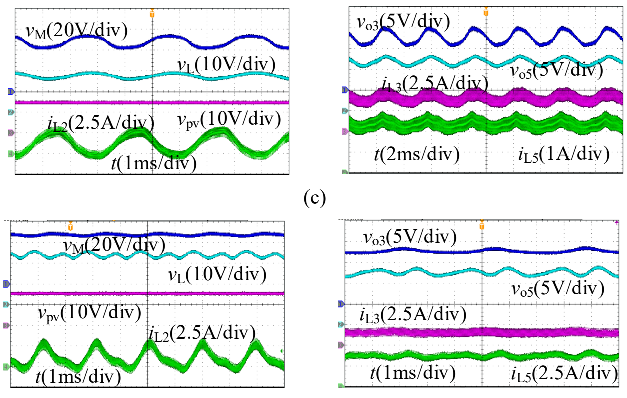

(d)

Fig. 15. Steady state experimental waveforms for MVdc bus and LVdc bus under different R_5 and R_3. (a) R_3 = 10 Ω, R_5 = 10 Ω. (b) R_3 = 5 Ω, R_5 = 8 Ω. (c) R_3 = 3 Ω, R_5 = 5 Ω. (d) R_3 = 10 Ω, R_5 = 3 Ω.

Dynamic experimental waveforms are obtained by changing R_5 from 10 Ω to 3 Ω to demonstrate the system stability before and after a load variation, like shown in Fig. 16. As can be seen, when the load is 10 Ω, the system is stable while bus voltages cannot be regulated stably and oscillations show up after stepping to 3 Ω.

It is concluded that the experimental results are corresponding to the obtained results of the proposed stability evaluation method.

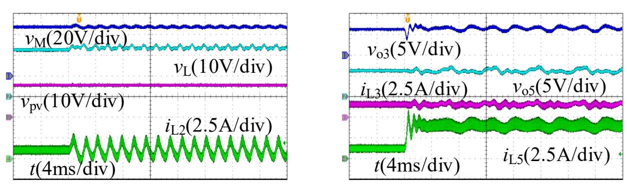

Fig. 16. Dynamic experimental waveforms for MVdc bus and LVdc bus when R_5 steps from 10 Ω to 3 Ω.

To make a better clarification for the features of the proposed stability criterion, TABLE III is given to compare some classic impedance-based stability methods. The impedance-based methods are widely used by scholars and researchers. The criteria using forbidden regions based on the Nyquist stability criterion are testing the Bode plots of individual impedances of subsystems to evaluate the stability for cascaded system, and the precondition is that there is no RHP pole in the minor loop gain. The impedance sum criteria based on Cauchy's Argument Principle, test the RHP pole in whole system's closed-loop characteristic polynomial. In this method, assuming there is no RHP pole in each subsystem, the stability can be assessed by checking the RHP zero of impedance sum. It can be known from [23 - 25] that the power electronic system can be categorized as $Z + Y$ system, $Z + Z$ system, $Y + Y$ system. For $Z + Y$ system, there should be no RHP pole in subsystems to meet the precondition that the minor loop gain ZY has no RHP pole. For $Z + Z$ system and $Y + Y$ system, there should be no RHP pole and zero in subsystems because the minor loop gains are Z/Z and Y/Y. Therefore, there are constraints of RHP pole and zero on subsystems if the criteria based on forbidden regions and impedance sum criteria are used. Moreover, these two methods analyze the simple system with direct power flow, with the increasing of system complexity, it will be more complicated.

[22] is an extension of criteria using forbidden regions which considers different power flow in dc distributed power system with single bus, providing a simple and general stability assessment. Since it is extended from the forbidden regions, the method in [22] is also assuming that there is no RHP pole in the impedance ratio. It is complex to analyze the stability of dc distributed power system with multiple buses because the existing of intermittent bus converter will introduce bi-direction power flow. Therefore, there are interactions of power converter in each distributed power system as well as interactions between different distributed power systems. Ref. [31] proposes an assessment method by using the general form in [22] to simplify the dc distributed power system with two buses. There are four kinds of input-to-output transfer functions based on different input variables with a total of twenty forms, which should be recalculated with the plug-and-play applications. Moreover, it is difficult to be extended with introduction of other buses because there are many operation modes for intermediate bus converters as well as high dimensionality. In the proposed method, the number of RHP pole of the open-loop transfer function for the system is considered in the criterion and there is no precondition so the stability of system consists of subsystems with RHP pole and zero can be analyzed correctly. Moreover, the stability of each bus port can be analyzed by checking the bode plots and zero-pole maps of impedances or admittances for each bus port. Therefore, by introducing extension unit, it is very easy to extend the method when other buses are connected. The lengthy process and tedious calculation for the adding bus ports are needed when it comes to investigate very complex system even though the method can be used.

TABLE III COMPARISONS

Methods	Criteria using forbidden regions [13-18]	Impedance sum criteria [23-25]	Impedance-based local stability criterion [22]	Impedance-based stability assessment methodology [31]	Proposed method
Configurations	Cascaded system with single bus	DC distributed power system with single bus	DC distributed power system with single bus	DC distributed power system with multiple buses	Multibus dc microgrid
Preconditions	Assuming fixed power flow and no RHP pole in the minor loop gain	Assuming no RHP pole in the impedance sum	Assuming no RHP pole in the impedance ratio	Assuming no RHP pole in the impedance ratio	Without constraints of RHP pole and zero on the subsystems
Advantages	Intuitive and effective for simple system	Intuitive and effective for simple system	Providing a simple and general stability assessment	Providing an effective way to analyze the stability of dc distributed power system with two buses	Stability of each bus can be evaluated separately; providing a very simple way to evaluate the stability of complex systems; easy to be extended
Disadvantages	Having constraints of RHP pole and zero on subsystems as well as power flow direction	Having constraints of RHP pole and zero on subsystems as well as power flow direction	Having constraints of RHP pole and zero on subsystems	Being high dimensionality, unsuitable for plug-and-play applications and complex to be extended	Lengthy process and tedious calculation are needed with analyzing very complex system

VI. CONCLUSIONS

In this paper, simplified forms for the multibus dc microgrid are discussed in detail. Then, based on the concept calculating the number N of times that the open-loop transfer function anti-clockwise encloses (-1, j0) by using bode plot instead of Nyquist diagram, a systemic stability evaluation method for the multibus dc microgrid is proposed, possessing simplicity and intuition. Experimental results indicate effectiveness of the proposed method. The research results of this stability evaluation method are concluded.

1) The stability method for multibus dc microgrid is applicable without any constraints on subsystems, i.e. there is no assumption that the subsystem should have no RHP pole and zero.
2) The stability of the multibus dc microgrid for each bus can be evaluated separately, providing a simple and new approach to evaluate the stability of complex systems. The impedances and admittances of the MVdc bus port and the LVdc bus port can be obtained, which are used to evaluate the stability of the MVdc bus as well as the LVdc bus respectively. It is concluded that with a relatively small load in MVdc bus port (or LVdc bus port), the oscillations in MVdc bus voltage (or LVdc bus voltage) will affect the LVdc bus voltage (or MVdc bus voltage). There is a stability interaction between different bus ports. And the bus port with the smaller load will suffer from more serious oscillations.
3) This paper focuses on the stability analysis of dc microgrid with two buses, which can be extended to more complex system. By adding extension units, the cluster of dc microgrids (multibus dc microgrid with many buses) can be investigated through checking bode plots and zero-pole maps of each bus port. Moreover, by taking out of the

extension unit, the single-bus dc microgrid can be analyzed using the proposed process. The proposed method can act as a generalized approach for investigating different configurations.

REFERENCES

[1] T. Dragičević, X. Lu, J. C. Vasquez, and J. M. Guerrero, "DC Microgrids-Part I: A Review of Control Strategies and Stabilization Techniques," *IEEE Trans. Power Electron.*, vol. 31, pp. 4876-4891, Jul. 2016.

[2] T. Dragičević, X. Lu, J. C. Vasquez, and J. M. Guerrero, "DC Microgrids-Part II: A Review of Power Architectures, Applications, and Standardization Issues," *IEEE Trans. Power Electron.*, vol. 31, pp. 3528-3549, May 2016.

[3] A. Hirsch, Y. Parag, and J. Guerrero, "Microgrids: A review of technologies, key drivers, and outstanding issues," *Renewable Sustain. Energy Rev.*, vol. 90, pp. 402-411, Mar. 2018.

[4] Y. Han, H. Li, P. Shen, E. A. A. Coelho, and J. M. Guerrero, "Review of active and reactive power sharing strategies in hierarchical controlled microgrids," *IEEE Trans. Power Electron.*, vol. 32, no. 3, pp. 2427-2450, Mar. 2017.

[5] S. Fang, Y. Wang, B. Gou, Y. Xu. "Towards future green maritime transportation: an overview of seaport microgrids and all-electric ships," *IEEE Trans. Veh. Technol.*, vol. 69, no. 1, pp. 6174-6185, Oct. 2020.

[6] K. Lai and L. Zhang, "Sizing and siting of energy storage systems in a military based vehicle-to-grid microgrid," *IEEE Trans. Ind. Appl*., doi: 10.1109/TIA.2021.3057339.

[7] D. Dong, I. Cvetkovic, D. Boroyevich, W. Zhang, R. Wang, and P. Mattavelli, "Grid-interface bidirectional converter for residential DC distribution systems-part one: high-density two-stage topology," *IEEE Trans. Power Electron.*, vol. 28, no. 4, pp. 1655-1666, Apr. 2013.

[8] T. Dragičević, J. C. Vasquez, J. M. Guerrero, and D. Skrlec, "Advanced LVDC electrical power architectures and microgrids: a step toward a new generation of power distribution networks," *IEEE Electrif. Mag.*, vol. 2, no. 1, pp. 54-65, Mar. 2014.

[9] N. Rashidirad, M. Hamzeh, K. Sheshyekani, and E. Afjei, "An effective method for low-frequency oscillations damping in multi-bus DC microgrids," *IEEE J. Emerg. Sel. Topics Circuits Syst.*, vol. 7, no. 3, pp. 403-412, Sep. 2017.

[10] R. R. Deshmukh, M. S. Ballal and H. M. Suryawanshi, "A fuzzy logic based supervisory control for power management in multibus dc microgrid," *IEEE Trans. Ind. Appl*., vol. 56, no. 6, pp. 6174-6185, Dec. 2020.

[11] N. Rashidirad, M. Hamzeh, K. Sheshyekani, and E. Afjei, "A simplified equivalent model for the analysis of low-frequency stability of multi-bus DC micro-grids," *IEEE Trans. Smart Grid*, vol. 9, no. 6, pp. 6170-6182, Nov. 2018.

[12] R. D. Middlebrook, "Input filter considerations in design and application of switching regulators," in *Proc. IEEE IAS*, 1976, pp. 366-382.

[13] C. M. Wildrick, "Stability of distributed power supply systems," M.S. thesis, Virginia Power Electron. Center, Virginia Tech., Blacksburg, VA, USA, Feb. 1993.

[14] A. Riccobono and E. Santi, "Comprehensive review of stability criteria for DC distribution systems," in *Proc. IEEE Energy Convers. Congr. Expo.*, 2012, pp. 3917-3925.

[15] X. Feng, J. Liu, and F. C. Lee, "Impedance specifications for stable dc distributed power systems," *IEEE Trans. Power Electron.*, vol. 17, no. 2, pp. 157-162, Mar. 2002.

[16] X. Feng, Z. Ye, K. Xing, F. C. Lee, and D. Borojevic, "Individual load impedance specification for a stable dc distributed power system," in *Proc. 14th Annu. IEEE APEC Expo.*, 1999, pp. 923-929.

[17] S. D. Sudhoff, S. F. Glover, P. T. Lamm, D. H. Schmucker, and D. E. Delisle, "Admittance space stability analysis of power electronic systems," *IEEE Trans. Aerosp. Electron.*, vol. 36, no. 3, pp. 965-973, Jul. 2000.

[18] S. D. Sudhoff and J. M. Crider, "Advancements in generalized immittance based stability analysis of dc power electronics based distribution systems," in *Proc. IEEE ESTS*, 2011, pp. 207-212.

[19] A. Riccobono and E. Santi, "Comprehensive review of stability criteria for DC power distribution systems," *IEEE Trans. Ind. Appl.*, vol. 50, no. 5, pp. 3525-3535, Sep. 2014.

[20] Q. Tian, G. Zhou, M. Leng, G. Xu and X. Fan, "A non-isolated symmetric bipolar output four-port converter interfacing PV-Battery system," *IEEE Trans. Power Electron.*, doi: 10.1109/TPEL.2020.2983113.

[21] M. Farrokhabadi, C. Cañizares, J. Porco, E. Nasr, L. Fan, P. Araya, R. Tonkoski and *et al*, "Microgrid stability definitions, analysis, and examples," *IEEE Trans. Power Syst.*, vol. 35, no. 1, pp. 13-29, Jan. 2020.

[22] X. Zhang, X. Ruan, and C. K. Tse, "Impedance-based local stability criterion for DC distributed power systems," *IEEE Trans. Circuits Syst. I, Reg. Papers*, vol. 62, no. 3, pp. 916-925, Mar. 2015.

[23] F. Liu, J. Liu, H. Zhang, and D. Xue, "Stability issues of Z + Z type cascade system in hybrid energy storage system (HESS)," *IEEE Trans. Power Electron.*, vol. 29, no. 11, pp. 5846-5859, Nov. 2014.

[24] H. Liu, X. Xie, X. Gao, H. Liu, and Y. Li, "Stability analysis of SSR in multiple wind farms connected to series-compensated systems using impedance network model," *IEEE Trans. Power Syst.*, vol. 33, no. 3, pp. 3118-3128, May 2018.

[25] Q. Zhong and X. Zhang, "Impedance-sum stability criterion for power electronic systems with two converters/sources," *IEEE Access*, vol. 7, pp. 21254-21265, Jan. 2019.

[26] S. K. Sahoo, A. K. Sinha, and N. K. Kishore, "Control techniques in AC, DC, and hybrid AC–DC microgrid: A review," *IEEE J. Emerg. Sel. Topics Power Electron.*, vol. 6, no. 2, pp. 738-759, Jun. 2018.

[27] M. Lee, W. Choi, H. Kim, and B. Cho, "Operation schemes of interconnected DC microgrids through an isolated bi-directional DC-DC converter," in *Proc. IEEE Appl. Power Electron. Conf. Expo.*, 2015, pp. 2940-2945.

[28] J. Wang, C. Jin, and P. Wang, "A uniform control strategy for the interlinking converter in hierarchical controlled hybrid AC/DC microgrids," *IEEE Trans. Ind. Electron.*, vol. 65, no. 8, pp. 6188-6197, Aug. 2018.

[29] Y. Xia, W. Wei, M. Yu, X. Wang, and Y. Peng, "Power management for a hybrid AC/DC microgrid with multiple subgrids," *IEEE Trans. Power Electron.*, vol. 33, no. 4, pp. 3520-3533, Apr. 2018.

[30] J. Siegers, S. Arrua, and E. Santi, "Stabilizing controller design for multibus MVDC distribution systems using a passivity-based stability criterion and positive feed forward control," *IEEE J. Emerg. Sel. Topics Power Electron.*, vol. 5, no. 1, pp. 14-27, Mar. 2017.

[31] P. Pan, W. Chen, L. Shu, H. Mu, K. Zhang, M. Zhu and F. Deng, "An impedance-based stability assessment methodology for DC distribution power system with multivoltage levels," *IEEE Trans. Power Electron.*, vol. 35, no. 4, pp. 4033-4047, Apr. 2020.

[32] X. Li, L. Guo, Y. Li, C. Hong, Y. Zhang, Z. Guo, D. Huang and C. Wang, "Flexible interlinking and coordinated power control of multiple DC microgrids clusters," *IEEE Trans. Sustain. Energy*, vol. 9, no. 2, pp. 904-915, Apr. 2018.

[33] X. Wang, Y. Peng, J. Zhu, Y. Xia, M. Yu, H. Hu, H. Cai and W. Wei, "Decentralized impedance specifications for small-signal stability of DC distributed power systems," *IEEE J. Emerg. Sel. Topics Power Electron.*, vol. 5, no. 4, pp. 1578-1588, Dec. 2017.

[34] M. Vidyasagar, D. G. Meyer, and G. F. Franklin, "Some simplifications of the graphical Nyquist criterion," *IEEE Trans. Automat. Contr.*, vol. 33, no. 3, pp. 301-305, Mar. 1988.

[35] D. Lumbreras, E. L. Barrios, A. Urtasun, A. Ursúa, L. Marroyo, and P. Sanchis, "On the stability of advanced power electronic converters: The generalized Bode criterion," *IEEE Trans. Power Electron.*, vol. 34, no. 9, pp. 9247-9262, Sep. 2019.

[36] J. Samanes, A. Urtasun, E. Barrios, D. Lumbreras, J. Lopez, E. Gubia and P. Sanchis, "Control design and stability analysis of power converters: the MIMO generalized bode criterion," *IEEE J. Emerg. Sel. Topics Power Electron.*, vol. 8, no. 2, pp. 1880-1893, Jun. 2020.

[37] Y. Liao and X. Wang, "Impedance-based stability analysis for interconnected converter systems with open-Loop RHP poles," *IEEE Trans. Power Electron.*, vol. 35, no. 4, pp. 4388-4397, Apr. 2020.

[38] G. F. Franklin, J. D. Powell, and A. Emami-Naeini, *Feedback control of dynamic systems*. London, U.K.: Pearson Educ., 2015.

[39] T. Suntio, T Messo, J. Puukko, *Power electronic converters: dynamics and control in conventional and renewable energy applications*. Weinheim, Germany.: Wiley-VCH, 2017.

[40] A. Francés, R. Asensi, Ó. García, R. Prieto and J. Uceda, "Modeling electronic power converters in smart DC microgrids-an overview," *IEEE Trans. Smart Grid.*, vol. 9, no. 6, pp. 6274-6287, Nov. 2018.

Minrui Leng (S'18) received the B.S. degree in electrical engineering and automation from Southwest Jiaotong University, Chengdu, China, in 2014, where she is currently working toward the Ph.D. degree in the School of Electrical Engineering.

She has been a Visiting Ph.D. Student with the Department of Energy Technology, Aalborg University, Aalborg, Denmark, since 2019. Her research interests include small signal modelling and dynamical modeling of power converter, control techniques of power converter, stability of distributed power systems and model predictive control, cyber-attacks of dc microgids.

Guohua Zhou (S'10–M'12–SM'14) received the B.S. degree in electronic and information engineering and the M.S. and Ph.D. degrees in electrical engineering from Southwest Jiaotong University, Chengdu, China, in 2005, 2008, and 2011, respectively.
From March 2010 to September 2010, he was a Research Assistant with the Department of Electronic and Information Engineering, Hong Kong Polytechnic University, Kowloon, Hong Kong. From October 2010 to March 2011, he was a Visiting Scholar (also a Joint Ph.D. student) with the Center for Power Electronics Systems, Virginia Polytechnic Institute and State University, Blacksburg, VA, USA. He is currently a Professor with the School of Electrical Engineering, Southwest Jiaotong University. His current research interests include modulation and control techniques of power electronics systems, dynamical modeling and analysis of switching power converters, and renewable energy applications of power electronics.

Haoze Li received the B.S. degree in electrical engineering and automation from Yanshan University, Qinhuangdao, China, in 2019. He is currently working toward the M.S. degree in the School of Electrical Engineering,Southwest Jiaotong University. His research interests include LED constant current driver and control techniques of power converter.

Guodong Xu was born in Henan, China, in 1996, He received the B. S. degree in electrical engineering and automation from Huaqiao University, Xiamen, China, in 2018. He is currently working toward the M.S. degree in electrical engineering in the Southwest Jiaotong University, Chengdu, China. His current research interests include modeling and stability analysis of the cascaded system.

Frede Blaabjerg (S'86–M'88–SM'97–F'03) was with ABB-Scandia, Randers, Denmark, from 1987 to 1988. From 1988 to 1992, he got the PhD degree in Electrical Engineering at Aalborg University in 1995. He became an Assistant Professor in 1992, an Associate Professor in 1996, and a Full Professor of power electronics and drives in 1998. From 2017 he became a Villum Investigator. He is honoris causa at University Politehnica Timisoara (UPT), Romania and Tallinn Technical University (TTU) in Estonia.

His current research interests include power electronics and its applications such as in wind turbines, PV systems, reliability, harmonics and adjustable speed drives. He has published more than 600 journal papers in the fields of power electronics and its applications. He is the co-author of four monographs and editor of ten books in power electronics and its applications.

He has received 32 IEEE Prize Paper Awards, the IEEE PELS Distinguished Service Award in 2009, the EPE-PEMC Council Award in 2010, the IEEE William E. Newell Power Electronics Award 2014, the Villum Kann Rasmussen Research Award 2014, the Global Energy Prize in 2019 and the 2020 IEEE Edison Medal. He was the Editor-in-Chief of the IEEE TRANSACTIONS ON POWER ELECTRONICS from 2006 to 2012. He has been Distinguished Lecturer for the IEEE Power Electronics Society from 2005 to 2007 and for the IEEE Industry Applications Society from 2010 to 2011 as well as 2017 to 2018. In 2019-2020 he serves a President of IEEE Power Electronics Society. He is Vice-President of the Danish Academy of Technical Sciences too. He is nominated in 2014-2019 by Thomson Reuters to be between the most 250 cited researchers in Engineering in the world.

Tomislav Dragičević (S'09-M'13-SM'17) received the M.Sc. and the industrial Ph.D. degrees in Electrical Engineering from the Faculty of Electrical Engineering, University of Zagreb, Croatia, in 2009 and 2013, respectively. From 2013 until 2016 he has been a Postdoctoral researcher at Aalborg University, Denmark. From 2016 until 2020 he was an Associate Professor at Aalborg University, Denmark. Currently, he is a Professor at the Technical University of Denmark. He made a guest professor stay at Nottingham University, UK during spring/summer of 2018. His research interest is application of advanced control, optimization and artificial intelligence inspired techniques to provide innovative and effective solutions to emerging challenges in design, control and diagnostics of power electronics intensive electrical distributions systems and microgrids. He has authored and co-authored more than 300 technical publications (more than 150 of them are published in international journals, mostly in IEEE), 10 book chapters and a book in the field. He serves as an Associate Editor in the IEEE TRANSACTIONS ON INDUSTRIAL ELECTRONICS, in IEEE TRANSACTIONS ON POWER ELECTRONICS, in IEEE Emerging and Selected Topics in Power Electronics and in IEEE Industrial Electronics Magazine. Dr. Dragičević is a recipient of the Končar prize for the best industrial PhD thesis in Croatia, a Robert Mayer Energy Conservation award, and he is a winner of an Alexander von Humboldt fellowship for experienced researchers.